Supporting Information for "Radar sounding of subsurface water-ice in eastern Coprates and Capri Chasmata, Mars"

R. Noguchi[1], K. Ishiyama[1,2], A. Kumamoto[3], C. Uemura[4], Y. Kasaba[3], T. Usui[1,5], A. Oura[3], and D. Shoji[5]

[1]Institute of Space and Astronautical Science, Japan Astronautical Exploration Agency, 3-1-1 Yoshinodai, 252-5210, Sagamihara, Kanagawa, Japan

[2]National Institute of Technology, Tsuruoka College, 104 Sawada, Inooka, Tsuruoka, Yamagata 997-8511, Japan

[3]Tohoku University, Aramaki-Aza-Aoba 6-3, Aoba-ku, Sendai, Miyagi, 980-8578, Japan

[4]SOKENDAI (Graduate University for Advanced Studies), 3-1-1 Yoshinodai, Sagamihara, Kanagawa, 252-5210, Japan

[5]Earth-Life Science Institute, Tokyo Institute of Technology, 2-12-1 Ookayama, Meguro, Tokyo, 152-8550, Japan

Contents of this file

Additional Supporting Information (Files uploaded separately)

---

1. Figure S1. An example of (A and B: original, C and D: interpreted reflectances are marked) SHARAD radargrams and (E,F) surface clutter-simulated radargrams. The simulation method is shown in the supplementary information.

2. Figure S2. (A) Exposed stratigraphy on the wall, (B) its identified stratigraphy, and (C) its corresponding radargram at Point 2 in Fig.1. The thickness of each layer on the stratigraphic column (B) was measured on a HiRISE DTM (HI_038733_1670_042478_1670-ALIGN-DEM.tiff). (D) The echo level versus delay time (black line). Red and blue lines indicate sidelobe and sidelobe +10 dB.

3. Figure S3. Topography map of Coprates Chasma. Base of the upper map was created using HRSC MOLA Blended DEM (Fergason et al., 2018). Hatched boxes indicate tiny nameless valleys (A, B, and C). CTX mosaic of each valley is shown in lower maps.

4. Data S1. SHARAD observation list which was used in this study.

5. Data S2. Locations of identified SHARAD reflectors.

6. Data S3. HiRISE DTM used in this study.

Kirchhoff approximation method for the clutter simulation

The simulated radargrams were created using Mars digital elevation model (DEM) and spacecraft locations during SHARAD operation. Mars DEM was based on the MOLA Mission Experiment Gridded Data Records (https://pds-geosciences.wustl.edu/mgs/mgs-m-mola-5-megdr-l3-v1/mgsl_300x/meg128/). Their resolution was 128 pixel per degree. Spacecraft locations were from geometry table files in PDS data provided by the U.S. SHARAD team (https://pds-geosciences.wustl.edu/mro/mro-m-sharad-5-radargram-v1/mrosh_2001/data/geom/). Assuming Kirchhoff approximation, the elec-

tromagnetic field scattered from a rough surface can be calculated as the summation of the electromagnetic field scattered from local micro planes. Using Mars DEM, the Mars surface within 3 degrees of latitude and longitude from the spacecraft nadir point (S) were divided into micro square planes with horizontal size of 1/1280 degree of longitude and latitude (dS). Then we calculated the direction from spacecraft to micro plane eR, normal direction of micro plane n, distance from the spacecraft to micro plane R, incident magnetic field at micro plane H_i, and derived the scattered electric field E_s using the Franz formula for perfect electric conductor (PEC) plane

$$E_s = 2ikZ_0 \int_S e_R \times \{e_R \times (n \times H_i)\} \frac{\exp(ikR)}{4\pi R} dS \quad (1)$$

where k is wave number of the electromagnetic wave, and Z_0 is wave impedance (120π). In the above calculation, we only assumed a PEC rough surface without any subsurface reflectors for reduction of calculation. So, we should note that simulated radargrams only include surface echoes whose intensity is different from observation due to reflectance difference from the actual one. On the other hand, the surface echo patterns (distance to the reflection point on the surface, R) found in the simulated radargram are expected to be the same as those in the observed radargram.

Component calculation in the case of the dielectric constant of non-porous rock being 8

In converting dielectric constants to composition, we assumed the rock portion was non-porous basalt. In the main text, we applied a value which is shown as non-porous basalt (14.9, an average of 14.768 and 14.955 for Mauna Ulu basaltic lava, Rust et al., 1999)

since most of the observed rock on Mars has low-SiO_2 components which are comparable to basalt and andesite McSween et al., 2009. However, several previous studies applied a lower rock dielectric constant (e.g., 8 is applied in Bramson et al., 2015). Here we show the results of a component calculation in the case of the dielectric constant of non-porous rock being 8 to help to compare with other studies/fields.

At point 1 in area II, assuming that these layers are pore-filling ice regime, the value of the calculated dielectric constant ($\sim$3.4) is consistent with a rock-air mixture with 36.6 % porosity (possible value in general geologic materials, Todd and Mays2005) and a rock-air-ice mixture, for which the range of volume fraction of water-ice is 0 – 21.4 % (Fig.A1). This simply leads to a maximum of 25.7 km^3 of putative water-ice, though such a large volume of water-ice is not possible considering the stratigraphic setting (water-ice can exist in the topmost layer considering the possible emplacement of snow at 0.4 Ma) as shown in the discussion in the main text.

At point 2 in area III, assuming that these layers are pore-filling ice regime, the value of the calculated dielectric constant ($\sim$4.0) is consistent with a rock-air mixture with 28.8 % porosity (possible value in general geologic materials, Todd and Mays, 2005) and a rock-air-ice mixture, of which the range of the volume fraction of ice is 0 – 34.7 % (Fig.A1). This simply leads to a maximum of 85.8 km^3 of putative water-ice, though such a large volume of water-ice is not possible considering the stratigraphic setting as shown in the discussion in the main text.

Reference

Bramson, A.M., S. Byrne, N.E. Putzig, S. Sutton, J.J. Plaut, T.C. Brothers, and J.W. Holt, 2015, Widespread excess ice in Arcadia Planitia, Mars, *Geophys. Res. Lett.,* **42**(16), 6566–6574.

McSween, H.Y., G.J. Taylor, and M.B. Wyatt, 2009, Elemental composition of the Martian crust, *Science*, **324**(5928), 736–739.

Rust, A.C., J.K. Russell, and R.J. Knight, 1999, Dielectric constant as a predictor of porosity in dry volcanic rocks, *J. Volcanol. Geotherm. Res.*, **91**(1), 79–96.

Todd, D.K. and L.W. Mays, 2005, Groundwater hydrology, 3rd ed, pp 636.

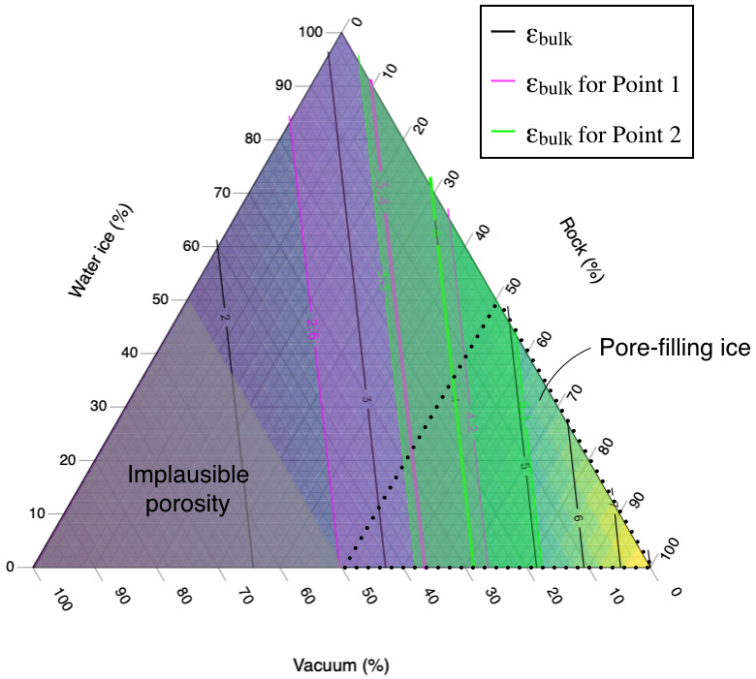

Figure A1. Ternary contour diagram of the bulk dielectric constant following the projection scheme of Bramson et al., 2015 using a dielectric constant of non-porous rock as 8. A gray triangle zone indicates implausible porosities. Dotted triangle shows pore-filling ice conditions.